Lead-free piezoelectric thin films for RoHS devices

Didier Fasquelle, Manuel Mascot, N. Sama, Denis Remiens, Jean-Claude Carru

Sensors and Actuators A 229 (2015) 30–35

Lead-free piezoelectric thin films for RoHS devices

D. Fasquelle [a,*], M. Mascot [a], N. Sama [b], D. Remiens [b], J.-C. Carru [a]

[a] UDSMM, Université du Littoral Côte d'Opale, 50 rue F. Buisson, BP717, 62228 Calais, France
[b] IEMN - DOAE, CNRS-UMR 8520, Université de Valenciennes et du Hainaut Cambrésis, Le Mont Houy, 59313, Valenciennes Cedex 9, France

Article info

Keywords:
BST
BTS
Thin films
Sol–gel
Piezoelectric

Abstract

This paper reports a study of $Ba_{0.9}Sr_{0.1}TiO_3$ and $BaTi_{0.98}Sn_{0.02}O_3$ thin films elaborated by a sol–gel route and deposited on Pt/Ti/SiO_2/Si substrates. These films were annealed at 950 °C and exhibited a polycrystalline structure. The AFM analysis revealed an important difference in the microstructure of the BST and BTS films. Our BTS film showed no significant piezoelectric properties as its coefficients were d_{33} = 5 pC/N and 4 pm/V for the direct and reverse measurements. Under our optimized annealing conditions, we gave the evidence that ferroelectric $Ba_{0.9}Sr_{0.1}TiO_3$ could be a good candidate to replace PZT in RoHS microelectronic devices, therefore for green applications where lead must be prohibited, and that, despite the factor 2 or 3 between coefficients measured on PZT and lead-free films.

1. Introduction

Piezoelectric actuators, infrared sensors, FeRAM usually contain lead based materials [1,2]. Among these materials, $PbZrTiO_3$ (PZT) is the most used thanks to its superior piezoelectric and ferroelectric properties. PZT is also remarkable for its high Curie temperature, i.e. its high ferroelectric-paraelectric phase transition [3]. However, its main disadvantage is in fact to contain lead in regards with the RoHS European directive (Restriction of Hazardous Substances). This recent directive prohibits different kinds of polluting materials like lead, mercury, cadmium, hexavalent chromium in electronic components. Lead is well known for its disastrous effects on the human nervous system. Lead is also responsible of the decrease of spermatozoon production, then influencing the human fertility. Lead has been so intensively used for centuries (for example, more than 2000 tons of lead were used in Europe in 2006) that it is now possible to find it in everything we eat like vegetables, fruits, meat and in a higher concentration in fish, crabs and seashells.

Accordingly, it is now necessary to implement materials without these prohibited or hazardous substances. From the perspective of thin films dedicated to piezoelectric applications, many lead-free materials have been studying quite recently. Guo et al. [4] measured the dielectric properties and piezoelectric cycles on $BaTiO_3$ films. Simoes et al. [5] have studied and published works on the ferroelectric and piezoelectric properties of $Bi_4Ti_3O_{12}$, $CaBi_4Ti_4O_{15}$ and $SrBi_4Ti_4O_{15}$ films. Niobate family is a way of interest as well. A ferroelectric $Na_{0.52}K_{0.48}NbO_3$ (NKN) thin film on Pt/Ti/SiO_2/Si substrate deposited by sputtering was characterized by the piezoelectric force microscopy [6]. (Bi,Na)TiO_3–(Bi,K)TiO_3–$BaTiO_3$ epitaxial thin films deposited on $SrRuO_3$ coated $SrTiO_3$ substrates exhibited an interesting transverse piezoelectric coefficient (e_{31},f) after poling [7]. Micro fabrications have been conducted for sodium potassium niobate [(K,Na)NbO_3, KNN] thin films by dry etching, where Pt/KNN/Pt unimorph micro cantilevers have been fabricated as a lead-free piezoelectric micro electro mechanical system (MEMS) [8]. Lead-free piezoelectric thick films (5–17 μm) of potassium sodium niobate with lithium antimonate $K_{0.5}Na_{0.5}$_NbO_3–$LiSbO_3$ have shown that thick films can be relevant candidates [9]. Recently, Barium titanate ($BaTiO_3$)–potassium niobate ($KNbO_3$) (BT–KN) nanocomplex ceramics with various KN/BT molar ratios were prepared by the solvothermal method, where samples were elaborated without any non-piezoelectric substrate [10].

Our work is dedicated to the study of $Ba_xSr_{1-x}TiO_3$ (BST) and $BaTi_{1-x}Sn_xO_3$ (BTS) thin films elaborated by a sol–gel route, which acts as potential lead-free candidates to replace PZT in various applications [11,12]. These materials were chosen because of their high dielectric constant and relatively weak losses. Moreover they present the advantage to exhibit an adjustable transition temperature between the paraelectric state and the ferroelectric state when changing the Ba/Sr ratio [3]. In this study, we focus on the piezoelectric properties of $Ba_{0.9}Sr_{0.1}TiO_3$ (BST 90/10) and $BaTi_{0.98}Sn_{0.02}O_3$ (BTS 98/2) thin films deposited on Pt/Si substrates by spin coating.

* Corresponding author. Tel.: +33 321465768; fax: +33 321465778.
E-mail address: didier.fasquelle@univ-littoral.fr (D. Fasquelle).

http://dx.doi.org/10.1016/j.sna.2015.02.009

These compositions define a Curie temperature higher than room temperature for applications in pyroelectric, ferroelectric and piezoelectric devices, which are however always lower than that of PZT [3]. And finally, we evaluate the potential of these lead-free materials for their applications in thin film RoHS devices.

2. Experimental details

The solutions were prepared from: alkaline acetates $Ba(CH_3COO)_2$, 99%, $Sr(CH_3COO)_2$ and Ti isopropoxide $Ti(C_{16}H_{28}O_6)$ for BST; alkaline acetates $Ba(CH_3COO)_2$, 99%, dibutyltin oxyde ($C_8H_{18}OSn$) and Ti isopropoxide $Ti(C_{16}H_{28}O_6)$ for BTS. Acetic acid ($C_2H_4O_2$) and 2-propanol ($CH_3CHOHCH_3$) were used as solvent agents. The complete route was previously described [13–15].

All films were deposited by a sol–gel process on commercial (100) silicon wafers with the following coatings: 1 μm SiO_2/40 nm Ti/200 nm Pt. Finally gold was evaporated through a shadow mask to realize the upper electrodes with circular dots ranging from 150 μm to 2 mm in diameter. The Pt layer acted as bottom electrode. The upper electrode diameter was measured by an Olympus BX60 optical microscope. The morphology of the films was determined using Scanning Electron Microscopy (SEM) with a LEO438 VP apparatus, and the grain size was directly measured with the software associated to the microscope. Atomic Force Microscopy (Multimode AFM, Vecco Instruments) was also used to determine the roughness of our films. The thickness of the films, which was either measured by SEM and with a TALYSURF INTRA 150 profilemeter, is close to 1 μm.

The piezoelectric properties were measured at room temperature. A home-made system was developed in our laboratory to measure the d_{33} piezoelectric coefficient by the direct method, inspired by the method introduced by Lefki et al. [16]. For the converse method, the d_{33} coefficient measurement is made by a single beam Mach–Zhender interferometer [17].

3. Results

3.1. Physical analysis

Fig. 1 shows the XRD patterns of the BST and BTS thin films annealed at 950 °C for 15 min. These annealing conditions have been optimized in previous works [13–15]. The films are well crystallized and the perovskite phase is identified. There is evidence that the growth is polycrystalline for all films with however a difference for the preferential orientation, which is (1 1 1) for the BST film and (1 1 0) for BTS.

Fig. 2 shows AFM photos of the BST film annealed at 950 °C for 15 min. Different sizes of grains are observed, ranging from 80 to 130 nm. But the average grain size of the BST film is about 110 nm, with a mean roughness of 3.5 nm. Moreover, these photos show a good density of regular grains and a smooth surface without holes between grains. Fig. 3 shows AFM photos of the BTS film annealed at 950 °C for 15 min. At first, with a look on the SEM photos (not presented here), we thought that the BTS thin film was made of bigger grains than those observed on the BST film. But the better resolution given by the AFM has revealed the right microstructure. In fact, the BTS film is made of big assemblies (blocks) of small grains ranging from 100 to 400 nm in length, and from 100 to 200 nm in width. Each block is composed of very small grains, which size varies from 10 to 30 nm. These big blocks also define a higher mean roughness of 7.2 nm, which is double than that measured on the BST film. Fig. 4 shows a 3D-view of AFM photos for the two thin films. The comparison of their microstructure is then easier: the BST film is composed of circular grains grown in a high density with thin boundaries, while the elongated blocks of the BTS film seem to be

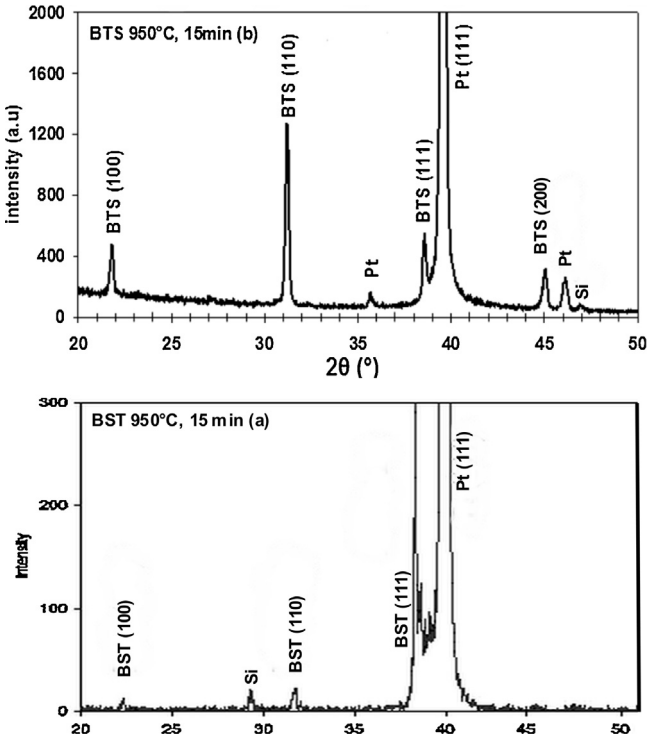

Fig. 1. XRD diagrams of the BST (a) and BTS (b) films annealed at 950 °C for 15 min.

the result of the growth of self-assembled pyramids with two main faces which define the block length. Therefore the block ridges are composed of peaks which are the small grains observed in Fig. 3. So thin boundaries can be distinguished between the very small grains, while deep boundaries appear between the elongated blocks.

Therefore, the microstructure of the BST and BTS films clearly corroborates the diffraction observations, as illustrated by the AFM photographs (Figs. 2 and 3). Indeed, for the BTS film, the growth competition is highlighted by a disturbed morphology where coexist three kinds of grains: pyramidal, elongated and rounded (Fig. 3). Each kind of grains corresponds to the different growth orientations: (1 0 0), (1 1 0) and (1 1 1), respectively. On the contrary, the BST film presents a more homogeneous and a well-organized microstructure than the BTS film. Indeed, the BST microstructure is characterized by the presence of rounded grains, which is completely in agreement with the (1 1 1)-oriented crystallites. The comparison between the two different kinds of microstructure is eased by the 3D-views given in Fig. 4. On each photograph, the analyzed area is 2 μm × 2 μm.

3.2. Piezoelectric properties

The converse piezoelectric effect describes the strain generated in a piezoelectric material in response to an applied electric field. This effect is written as:

$$S_i = d_{ij} \times E_j \quad (1)$$

where S_i is the induced strain, E_j is the applied electric field and d_{ij} is the piezoelectric coefficient. The piezoelectric coefficient, which is in fact a third rank tensor, can be written in Eq. (1) in reduced matrix notation by representing the mechanical strain as a 1-dimensional matrix with elements $i = 1, 2 \ldots 6$. This converse piezoelectric effect is then exploited in actuators for producing a displacement under a voltage control.

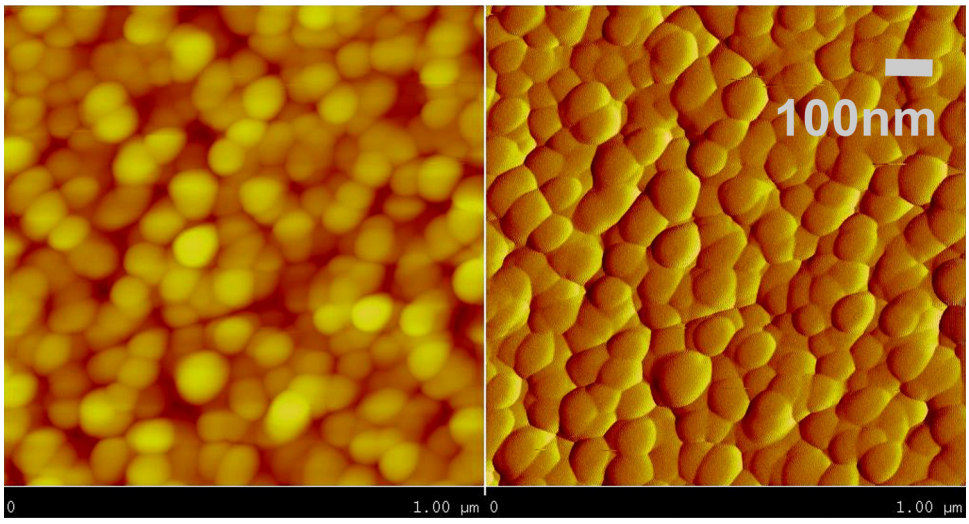

Fig. 2. AFM pictures of a BST film annealed in air at 950 °C for 15 min.

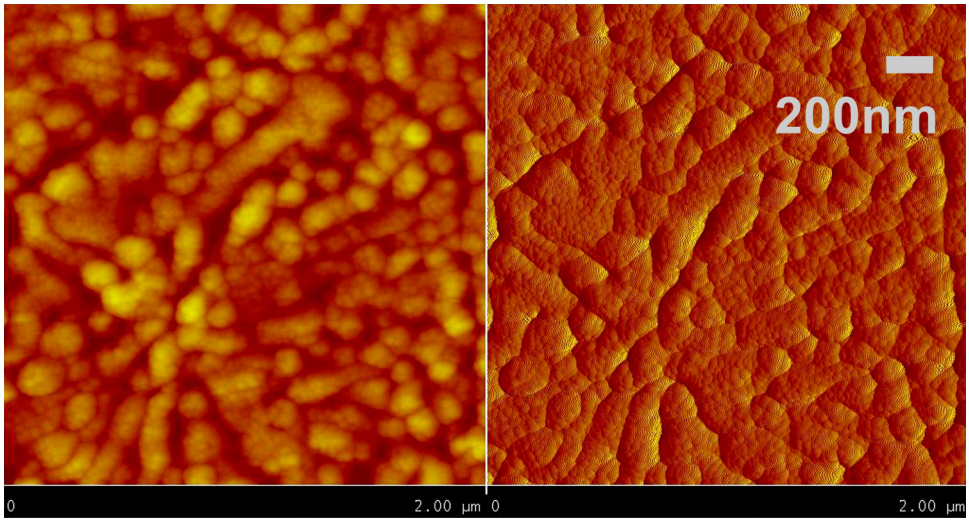

Fig. 3. AFM pictures of a BTS film annealed in air at 950 °C for 15 min.

For displacement sensors, the direct piezoelectric effect describes a change in polarization due to an applied stress and is written as:

$$D_i = d_{ij} \times s_j \tag{2}$$

where D_i is the dielectric displacement and σ_j is the applied stress.

In Eqs. (1) and (2), the coordinate axes are defined by the polarization of the sample and is assigned to the 3-direction. When an electric field is applied parallel to the 3-direction and the strain also measured in the 3-direction, the corresponding piezoelectric coefficient is the longitudinal piezoelectric coefficient, d_{33}:

$$S_3 = d_{33}E_3 \tag{3}$$

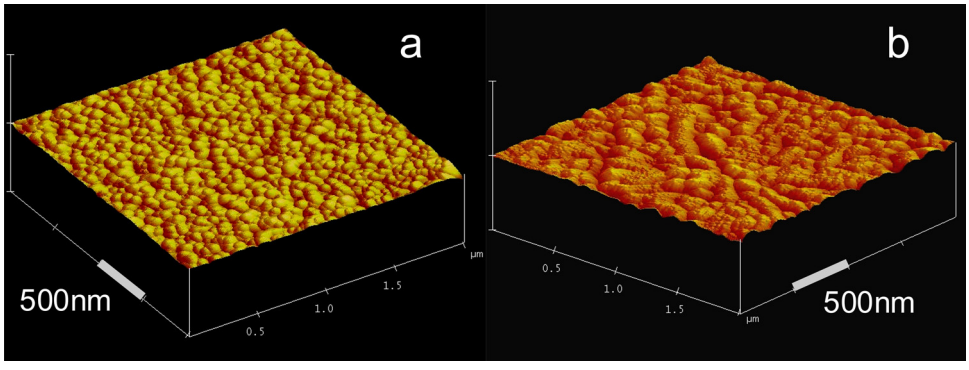

Fig. 4. 3D-view AFM photos given for the BST (a) and BTS (b) films.

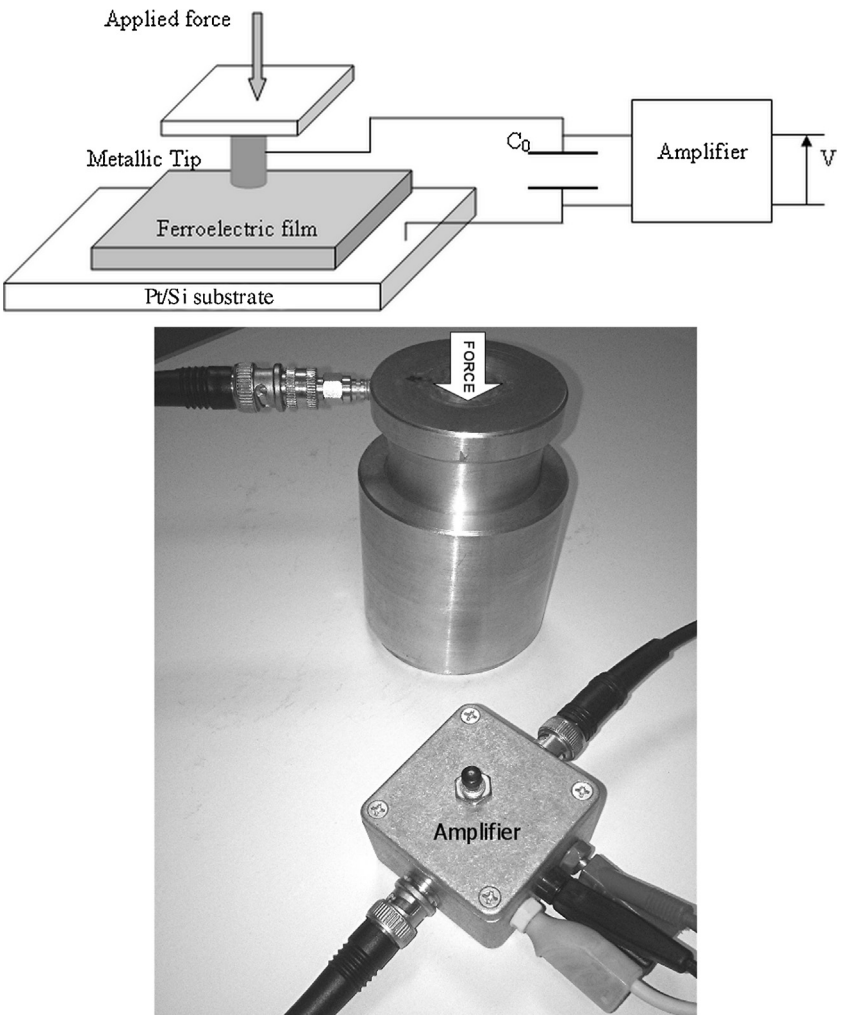

Fig. 5. Principle and photograph of our home-made set-up for the direct measurement of the d_{33} piezoelectric coefficient.

The piezoelectric coefficients described by the direct and converse piezoelectric effects are mathematically equivalent. Therefore, the longitudinal piezoelectric coefficient described by the converse piezoelectric effect (Eq. (3)) is equivalent to the longitudinal piezoelectric coefficient described by the direct piezoelectric effect:

$$D_3 = d_{33} \times s_3 \tag{4}$$

Our home-made set-up used for the electrical charge measurement and extraction of the direct piezoelectric coefficient is presented in Fig. 5. The obtained macroscopic response for the BST film, which was linear in our 1–10 N force range, is presented in Fig. 6. The measured coefficient is $d_{33\text{eff}} = 19$ pC/N. As the d_{33} value of PZT thin films can be as high as 101 pC/N [18], but not measured in the same conditions than our BST film, our result remains interesting as the goal is to eliminate lead in piezoelectric applications. An additional consideration must be given here as the piezoelectric properties of our BST films might be improved by optimizing the material, increasing the thickness, poling the ferroelectric layer to line up more ferroelectric domains in the same direction or adding a buffer layer. On the BTS film, the recorded values were really lower, as our maximum value was 5 pC/N. This result, which definitely confirms that BTS cannot be used for piezoelectric devices, can be linked to the growth competition highlighted previously in the text, where three kinds of grains coexist in a disturbed morphology as seen in Figs. 3 and 4. In fact, the ferroelectric properties of the BTS film were also weak as indicated in Table 1.

We have also measured in this work the converse piezoelectric coefficient by a single beam interferometer, an alternative and simple method to overcome the complexity of using a two beam interferometer. The experimental arrangement used consists of a modified Laser Doppler Vibrometer which is combined with a Nikon optical microscope for beam delivery to the sample. The vibrometer delivers the measurement beam via a fibre optic link.

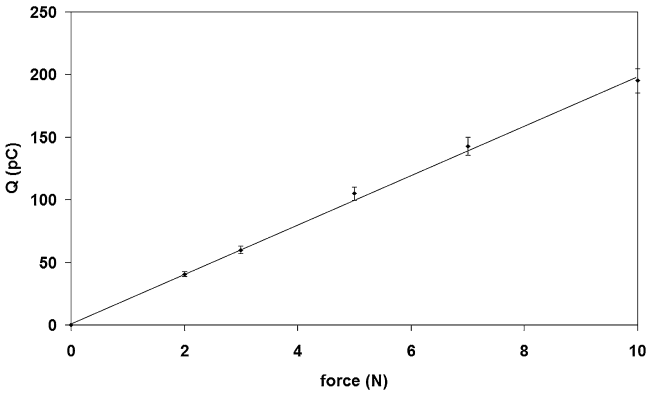

Fig. 6. Evolution of the electric charge in function of the applied force given for the BST thin film.

Table 1
Electrical properties of our $Ba_{0.9}Sr_{0.1}TiO_3$ and $BaTi_{0.98}Sn_{0.02}O_3$ thin films. Properties of other films (labelled *** and already published [13–15]) are given here for comparison.

	ε' (1 MHz)	$t_g\delta$ (1 MHz)	d_{33} (pC/N)	γ (μC/m^2/K)	Pr (μC/cm^2)
$BST_{750\,^\circ C\text{-}1h}$***	330	0.006			1
$BST_{950\,^\circ C\text{-}15min}$	780	0.015	19	340	13
$BTS_{750\,^\circ C\text{-}1h}$***	525	0.012			2
$BTS_{950\,^\circ C\text{-}15min}$	820	0.026	5	140	3.5

An adjustment stage facilitates positioning and focusing of the measurement beam on the sample surface. The probing focused laser spot has a typical size of around 15 μm. The resolution of the system is 2 pm and the band width is 2 MHz (between [1 Hz, 2 MHz]). The sample (including electrodes) and the focused laser spot are monitored via a video microscope and video monitor. With this experimental set-up it is possible to measure the piezoelectric hysteresis loops. A typical example is shown in Fig. 7.

As the piezoelectric cycles present a light shift due to the different kinds of electrodes, we have calculated a piezoelectric mean value by:

$$d_{33}\,m = (+d_{33} - (-d_{33}))/2 \quad (5)$$

when the electric field is null.

The BST film gave a d_{33} value of 21 pm/V, while the value was 4 pm/V for BTS. The observed difference between these results is of the same order than that given by the direct piezoelectric coefficients. For comparison, the same measurement conducted on a Sol–Gel PZT film [19] gave a d_{33} value of 26 pm/V, which confirms the great interest in ferroelectric BST films. Indeed, this d_{33} value measured on our $Ba_{0.9}Sr_{0.1}TiO_3$ film is interesting for a lead-free thin film when compared to relevant results. Guo et al. [4] measured a d_{33} mean value of 30 pm/V on an (1 0 0)-oriented $BaTiO_3$ film deposited on a Pt/Si substrate covered by a $LaNiO_3$ layer, but this good value was obtained by a local measurement, i.e. piezoresponse mode of AFM (PFM). In fact, individual grains excited by a PFM tip can show really higher values of the remnant d_{33}. Simoes et al. [5] measured an encouraging d_{33} value of 20 pm/V for a $CaBi_4Ti_4O_{15}$ film. Ferroelectric $Na_{0.52}K_{0.48}NbO_3$ (NKN) thin film on Pt/Ti/SiO_2/Si substrate, which was prepared using a radio frequency magnetron sputtering method, has given a piezoelectric constant d_{33} of about 45 pm/V using the piezoelectric force microscopy [6]. (Bi,Na)TiO_3–(Bi,K)TiO_3–$BaTiO_3$ epitaxial thin films deposited on $SrRuO_3$ coated $SrTiO_3$ substrates exhibited a transverse piezoelectric coefficient (e_{31},f) after poling at 600 kV/cm of $-2.2\,^\circ C/m^2$ [7]. Starting from the displacement of the Pt/KNN/Pt micro cantilevers, piezoelectric coefficients d_{31} of the KNN thin film were estimated to be 99–219 pm/V [8]. But the MEMS mechanism is well known for its ability of producing higher displacement than a film clamped to a substrate. Lead-free piezoelectric thick films (5–17 μm) of potassium sodium niobate with lithium antimonate $K_{0.5}Na_{0.5}$-NbO_3–$LiSbO_3$ have given a d_{33} of 50 pm/V [9]. With a KN layer thickness of the BT–KN nanocomplex ceramics ranging from 5 to 45 nm, the apparent piezoelectric constant d_{33} has shown values ranging from 80 to 170 pm/V [10]. But this kind of sample structure, i.e. without any non-piezoelectric substrate, exhibits a completely different behaviour. It is worth to note here that most of piezoelectric measurements made on thin films are related to the inverse effect and local measurements obtained by PFM, such as references given here. So it is not really easy to compare piezoelectric results obtained on lead-free thin films as we have chosen here to only make macroscopic measurements by the direct and converse piezoelectric techniques. And finally the choice done here to compare films all elaborated by sol–gel and deposited by spin coating on Pt/Si substrates, has really given a good opportunity to compare

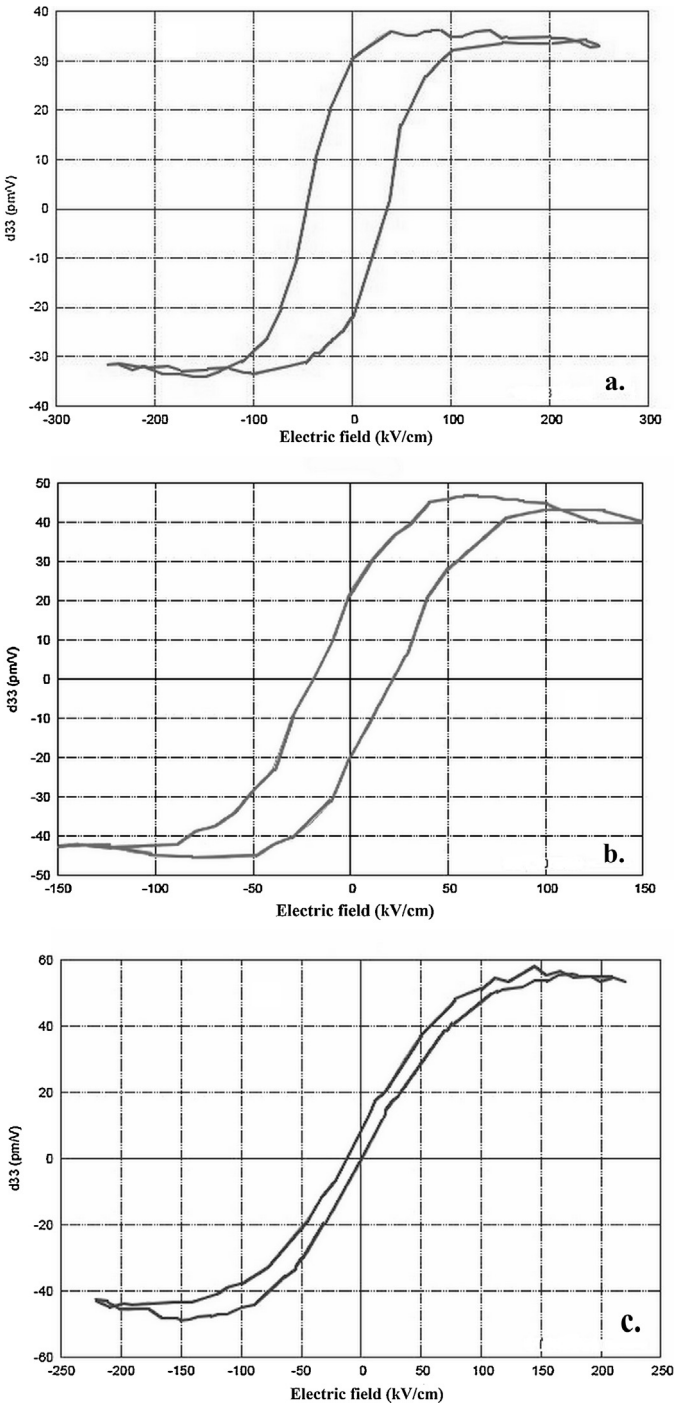

Fig. 7. Evolution of the piezoelectric coefficient d_{33} in function of the electric field, given for a PZT film (a), a BST film (b) and a BTS film (c). All these measurements were done in the same conditions on the different films.

PZT and BST responses in a good way as the same technique was applied to the different samples for the d_{33} measurements.

Despite the different techniques of measurement, we can nevertheless conclude that there is not so far any lead-free candidate to replace PZT or PMN-PT in power piezoelectric applications like actuators or sonar sensors. For microactuators, i.e. applications of piezoelectric thin films, we have currently a factor 2 or 3 between coefficients measured on PZT and lead-free films, when compared the d_{33} coefficient of thin films. Finally all these results show that lead-free ferroelectric materials, even dedicated to thin films' applications like sensors or micro-devices, can be nevertheless

considered as real challengers for PZT replacement in RoHS devices and green applications, except for power piezoelectric applications. Actually many studies run to find the "ideal" lead-free candidate that might be used in various piezoelectric applications, including high temperature ranges where the material needs to possess a high Curie temperature, i.e. a high paraelectric to ferroelectric transition temperature.

4. Conclusions

$Ba_{0.9}Sr_{0.1}TiO_3$ and $BaTi_{0.98}Sn_{0.02}O_3$ thin films were deposited by a classical sol–gel process on silicon substrates covered by a 200 nm platinum layer. Due to its non-significant piezoelectric properties, BTS cannot be considered as a potential candidate for piezoelectric applications. Under our optimized annealing conditions (950 °C for 15 min), we gave the evidence that ferroelectric $Ba_{0.9}Sr_{0.1}TiO_3$ is a real challenger to replace PZT in various integrated applications. In fact, as the piezoelectric properties measured on our BST thin films were particularly significant, we assume that $Ba_{0.9}Sr_{0.1}TiO_3$ may be used in RoHS microelectronic devices, therefore for green applications where lead must be prohibited.

References

[1] M.A. Dubois, P. Muralt, Measurement of the effective transverse piezoelectric coefficient $e_{31,f}$ of AlN and $Pb(Zr_x.Ti_{1-x})O_3$ thin films, Sens. Actuators 77 (1999) 106–112.

[2] Yi-Chu Hsu, Chia-Che Wu, Cheng-Chun Lee, G.Z. Cao, I.Y. Shen, Demonstration and characterization of PZT thin-film sensors and actuators for meso- and micro-structures, Sens. Actuators A116 (2004) 369–377.

[3] B. Jaffe, W.R. Cook Jr., H. Jaffe, Academic Press, London, New York, 1971, pp. 185–212.

[4] Y. Guo, K. Suzuki, K. Nishizawa, T. Miki, K. Kato, Dielectric and piezoelectric properties of highly (1 0 0)-oriented $BaTiO_3$ thin film grown on a $Pt/TiO_x/SiO_2/Si$ substrate using $LaNiO_3$ as a buffer layer, J. Cryst. Growth 284 (2005) 190–196.

[5] A.Z. Simoes, C.S. Riccardi, A. Ries, M.A. Ramirez, E. Longo, J.A. Varela, Ferroelectric and piezoelectric properties of bismuth layered thin films grown on (1 0 0) Pt electrodes, J. Mater. Process. Technol. 196 (2008) 10–14.

[6] Hai Joon Lee, Ill Won Kim, Jin Soo Kim, Chang Won Ahn, Bae Ho Park, Ferroelectric and piezoelectric properties of $Na_{0.52}K_{0.48}NbO_3$ thin films prepared by radio frequency magnetron sputtering, Appl. Phys. Lett. 94 (2009) 092902.

[7] M. Abazari, A. Safari, S.S.N. Bharadwaja, S. Trolier-McKinstry, Dielectric and piezoelectric properties of lead-free $(Bi,Na)TiO_3$-based thin films, Appl. Phys. Lett. 96 (2010) 082903.

[8] F. Kurokawa, R. Yokokawa, H. Kotera, F. Horikiri, K. Shibata, T. Mishima, M. Sato, I. Kanno, Micro fabrication of lead-free $(K,Na)NbO_3$ piezoelectric thin films by dry etching, Micro Nano Lett. 7 (12) (2012) 1223–1225.

[9] Jungho Ryu, Jong-Jin Choi, Byung-Dong Hahn, Dong-Soo Park, Woon-Ha Yoon, Ferroelectric and piezoelectric properties of $0.948K_{0.5}Na_{0.5}NbO_3$-$0.052LiSbO_3$ lead-free piezoelectric thick film by aerosol deposition, Appl. Phys. Lett. 92 (2008) 012905.

[10] Satoshi Wada, Kenta Yamashita, Ichiro Fujii, Kouichi Nakashima, Nobuhiro Kumada, Chikako Moriyoshi, Yoshihiro Kuroiwa, Enhanced piezoelectric properties of barium titanate–potassium niobate nano-structured ceramics by MPB engineering, Ceram. Int. 39 (Suppl. 1) (2013) 97–102.

[11] Hong Zhu, Jianmin Miao, Minoru Noda, Masanori Okuyama, Preparation of BST ferroelectric thin film by metal organic decomposition for infrared sensor, Sens. Actuators A110 (2004) 371–377.

[12] H.V. Alexandru, C. Berbecaru, F. Stanculescu, A. Ioachim, M.G. Banciu, M.I. Toacsen, L. Nedelcu, D. Ghetu, G. Stoica, Ferroelectric solid solutions $(Ba,Sr)TiO_3$ for microwave applications, Mater. Sci. Eng. B118 (2005) 92–96.

[13] M. Mascot, D. Fasquelle, G. Velu, A. Ferri, R. Desfeux, L. Courcot, J.-C. Carru, Pyro, ferro and dielectric properties of $Ba_{0.8}Sr_{0.2}TiO_3$ films deposited by Sol–Gel on platinized silicon substrates, Ferroelectrics 362 (2008) 79–86.

[14] D. Fasquelle, M. Mascot, J.-C. Carru, Electrical properties optimization of $Ba_{0.9}Sr_{0.1}TiO_3$ thin films deposited by sol–gel, Adv. Mater. Res. 277 (2011) 1–10.

[15] M. Mascot, D. Fasquelle, J.-C. Carru, Very high tunability of $BaSn_xTi_{1-x}O_3$ ferroelectric thin films deposited by sol–gel, Funct. Mater. Lett. 4 (1) (2011) 49–52.

[16] K. Lefki, G.J.M. Dormans, Measurement of piezoelectric coefficients of ferroelectric thin films, J. Appl. Phys. 76 (1994) 1764–1767.

[17] R. Herdier, D. Jenkins, E. Dogheche, D. Rèmiens, M. Sulc, Laser Doppler vibrometry for evaluating the piezoeletric coefficient d_{33} of thin film, Rev. Sci. Instrum. 77 (2006) 093905.

[18] W. Ren, H.J. Zhou, Measurement of piezoelectric coefficients of zirconate titanate thin films by the normal load method using a composite, Mater. Lett. 31 (1997) 185–188.

[19] M. Mascot, Thesis of University of Littoral Côte d'Opale, Calais, France, 2009.